

Research Article

Human serine racemase is allosterically modulated by NADH and reduced nicotinamide derivatives

Stefano Bruno^{1*}, Francesco Marchesani^{1,*}, Luca Dellafiora², Marilena Margiotta¹, Serena Faggiano¹, Barbara Campanini¹ and Andrea Mozzarelli^{1,3,4}

¹Department of Pharmacy, University of Parma, Parma, Italy; ²Department of Food Science, University of Parma, Parma, Italy; ³Institute of Biophysics, CNR, Pisa, Italy; and ⁴National Institute of Biostructures and Biomolecules, Rome, Italy

Correspondence: Stefano Bruno (stefano.bruno@unipr.it)

Serine racemase catalyzes both the synthesis and the degradation of D-serine, an obligatory co-agonist of the glutamatergic NMDA receptors. It is allosterically controlled by adenosine triphosphate (ATP), which increases its activity around 7-fold through a co-operative binding mechanism. Serine racemase has been proposed as a drug target for the treatment of several neuropathologies but, so far, the search has been directed only toward the active site, with the identification of a few, low-affinity inhibitors. Following the recent observation that nicotinamide adenine dinucleotide (reduced form) (NADH) inhibits serine racemase, here we show that the inhibition is partial, with an IC_{50} of $246 \pm 63 \mu\text{M}$, several-fold higher than NADH intracellular concentrations. At saturating concentrations of NADH, ATP binds with a 2-fold lower affinity and without co-operativity, suggesting ligand competition. NADH also reduces the weak activity of human serine racemase in the absence of ATP, indicating an additional ATP-independent inhibition mechanism. By dissecting the NADH molecule, we discovered that the inhibitory determinant is the N-substituted 1,4-dihydronicotinamide ring. Particularly, the NADH precursor 1,4-dihydronicotinamide mononucleotide exhibited a partial mixed-type inhibition, with a K_i of $18 \pm 7 \mu\text{M}$. Docking simulations suggested that all 1,4-dihydronicotinamide derivatives bind at the interdimeric interface, with the ring positioned in an unoccupied site next to the ATP-binding site. This newly recognized allosteric site might be exploited for the design of high-affinity serine racemase effectors to finely modulate D-serine homeostasis.

Introduction

The activation of the glutamatergic N-methyl D-aspartate receptors (NMDARs) requires the binding of either glycine or D-serine, two obligatory co-agonists competing for the same binding site [1]. Human serine racemase (EC 5.1.1.18, hSR) [2–8] is the homodimeric pyridoxal 5'-phosphate (PLP)-dependent enzyme that catalyzes both the reversible racemization of L-serine to D-serine and the irreversible β -elimination of L- and D-serine to pyruvate and ammonia [3,4,9]. Both reactions contribute to D-serine homeostasis, with the former producing and the latter removing D-serine, in conjunction with D-amino acid oxidase (DAAO), the main degradative enzyme for D-amino acids [10]. hSR is mostly localized in neurons and astrocytes [11,12], but also in other cells in peripheral tissues [13].

The impairment of NMDAR-mediated neurotransmission has been linked to several neuropathologies [14], with the hyperfunction associated with amyotrophic lateral sclerosis and Alzheimer's and Parkinson's diseases, and the hypofunction associated with schizophrenia. As direct NMDAR targeting with drugs such as memantine and ketamine produces excitotoxicity [15,16], the modulation of D-serine biosynthesis by hSR has been proposed as an alternative and milder pharmacological approach [17,18]. However, despite several attempts at designing inhibitors directed toward the active site, only a few have been identified, with K_i s in the high micromolar to millimolar range [19–26].

*These authors contributed equally to this work.

Received: 10 June 2016
Revised: 3 August 2016
Accepted: 4 August 2016

Accepted Manuscript online:
4 August 2016
Version of Record published:
11 October 2016

The best inhibitor identified so far is 2,2-dichloromalonate, with a K_i of 19 μM [23]. As malonate [27], it binds in a small pocket of the active site and exhibits limited possibilities for further optimization.

Recently, it was reported that nicotinamide adenine dinucleotide (reduced form) (NADH) inhibits hSR, suggesting a physiological regulation of hSR activity by the glycolytic flux in neurons [28]. Here, we thoroughly investigated the inhibition of hSR by NADH and by some of its analogues, derivatives and metabolic precursors. Indeed, some of the NADH precursors formed in the kynurenine pathway are involved in the glutamatergic neurotransmission, including kynurenic acid (KYNA) [29], quinolinic acid (QUIN) [30], 3-hydroxykynurenine (3-HK) [31] and xanthurenic acid (XA) [32]. More recently, the NADH metabolic precursor nicotinamide mononucleotide (NMN) was shown to accumulate after nerve injury — reaching intracellular concentrations in the micromolar range — and to promote axon degeneration [33].

Results and discussion

Inhibition of hSR by reduced NADH and NADPH

The effect of NADH, nicotinamide adenine dinucleotide (oxidized form) (NAD^+), NADPH and NADP^+ was tested on the racemization and β -elimination activities of hSR in the presence of 50 mM L-serine, 2 mM ATP, 2 mM MgCl_2 and 2 mM of each dinucleotide (Figure 1). NADH and NADPH reduced the racemization activity by about 50% and the β -elimination activity by about 36%. The difference can be ascribed to the nonnegligible inhibition on the β -elimination activity exerted by the NADH present in the coupled assay (vide infra). This limited inhibition by NADH at millimolar concentrations is consistent with recently reported observations [28]. The oxidized forms NAD^+ and NADP^+ did not produce any significant changes in hSR activity (Figure 1). The inhibition did not depend on the incubation time of hSR with NADH, nor on the presence of reducing agents, such as tris(2-carboxyethyl)phosphine (TCEP) or dithiothreitol (data not shown).

The structural similarity of NADH and ATP — which activates hSR about 7-fold in a co-operative fashion [9] — suggested a competition for the same binding site, with NADH binding counteracting ATP activation. Indeed, the binding properties of ATP in the presence of 2 mM NADH changed significantly. The K_D increased from 168 ± 12 to 370 ± 30 μM , with a complete loss of co-operativity (Supplementary Figure S1). However, a 20-fold excess of ATP with respect to NADH led only to a partial recovery of enzyme activity (Supplementary Figure S1), suggesting that NADH cannot be fully displaced. NAD^+ did not seem to compete at all with NADH (Supplementary Figure S1). The inhibition did not depend significantly on the order in which ATP and NADH were added to the assay mixture (Supplementary Figure S2). The slightly lower activity measured upon preincubation with ATP at 37°C and at pH 8.0 might be due to the partial hydrolysis of the activator ATP.

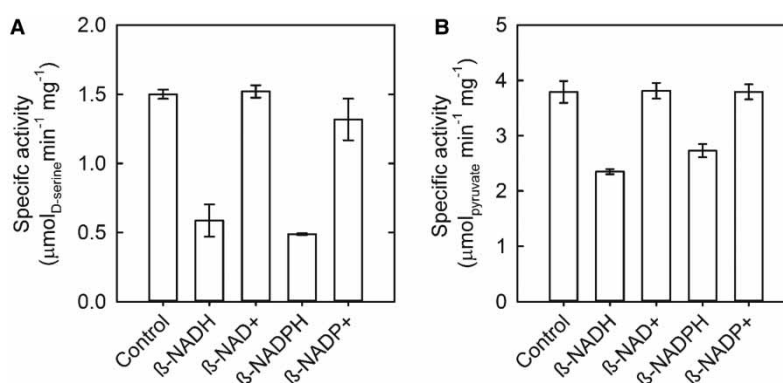


Figure 1. Inhibition of hSR by NADH and NADPH.

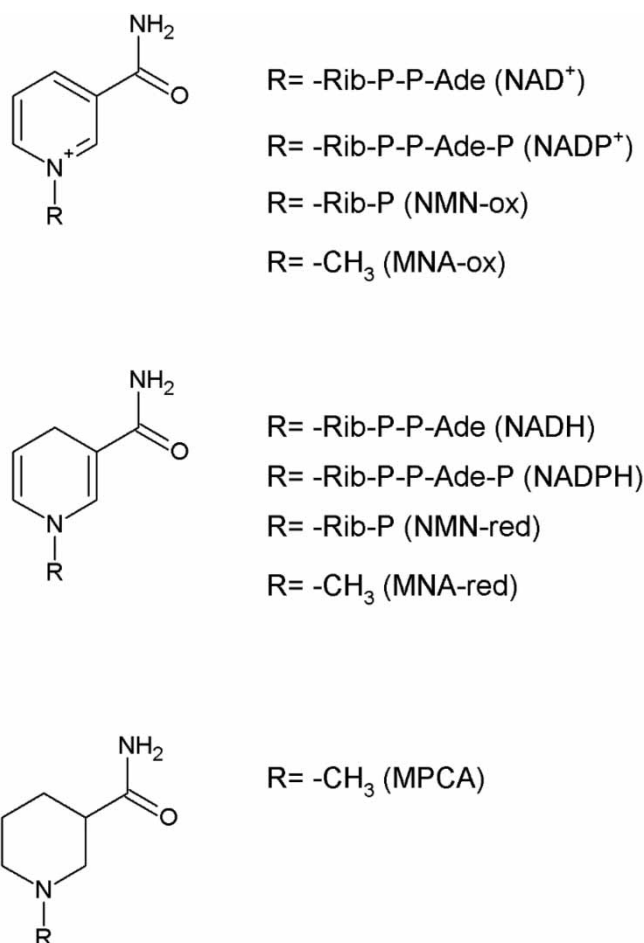
(A) Effect of NADH, NAD^+ , NADPH and NADP^+ on L-serine racemization activity. The control experiment was carried out by incubating 1.5 μM hSR in a 50 mM TEA-buffered solution containing 50 mM L-serine, 2 mM ATP- Mg^{2+} at a pH of 8.0. NAD^+ , NADH, NADP^+ or NADPH were added at a concentration of 2 mM. The error bars are the s.e.m. of two replicates. (B) Effect of NADH, NAD^+ , NADPH and NADP^+ on the L-serine β -elimination reaction. The reference experiment was carried out by incubating 0.45 μM hSR in a TEA-buffered solution containing 50 mM L-serine, 2 mM ATP and 2 mM MgCl_2 . NAD^+ , NADH, NADP^+ and NADPH were added at a concentration of 2 mM. The error bars are the s.e.m. of two replicates.

Identification of the inhibitory determinant of NADH

The NADH/NAD⁺ fragments 1-methyl-1,4-dihydronicotinamide (MNA-red), 1,4-dihydronicotinamide mononucleotide (NMN-red), their oxidized forms 1-methylnicotinamide (MNA-ox) and β-nicotinamide mononucleotide (NMN-ox), the fully reduced form of MNA-ox–1-methyl 3-piperidinecarboxamide (MPCA; Scheme 1), adenosine diphosphate (ADP) and sodium pyrophosphate were screened at 2 mM concentration using the β-elimination assay to identify the inhibitory determinant of NADH (Figure 2). ADP did not bring about any inhibition, as had emerged already [3]. Pyrophosphate ions at 2 mM concentration produced an inhibition of around 60%, which has been already associated with Mg²⁺ chelation [34]. Indeed, addition of an excess of Mg²⁺ fully reversed the inhibition (Supplementary Figure S3), whereas it did not have any effect on the inhibitory activity of the other compounds. Consistent with this proposed mechanism, the dependence of the activity of hSR on the concentration of sodium pyrophosphate was biphasic (Supplementary Figure S3), reflecting the scavenging of Mg²⁺ ions from both the ATP-Mg²⁺-binding site and the Mg²⁺/Ca²⁺-binding site. NMN-red and MNA-red inhibited hSR by 46% and 25%, respectively (Figure 2).

Overall, it can be concluded that the inhibition determinant of NADH is the N-substituted 1,4-dihydronicotininic ring. The redox state of the 1,4-dihydronicotininic ring is crucial, as neither the oxidized forms (NAD⁺, NADP⁺, NMN-ox and MNA-ox) nor the fully reduced piperidinic form (MPCA) showed any inhibitory activity. The redox forms of the nicotinamidic ring differ both in net charge and conformation, offering indications on the binding properties of the pocket.

To further explore the structural determinants of NADH binding to hSR, nicotinamide (Nam), its analogues nicotinic acid and isoniazid, as well as intermediates of the NADH-producing kynurenine pathway — tryptophan,



Scheme 1. Nam derivatives tested in the present study.

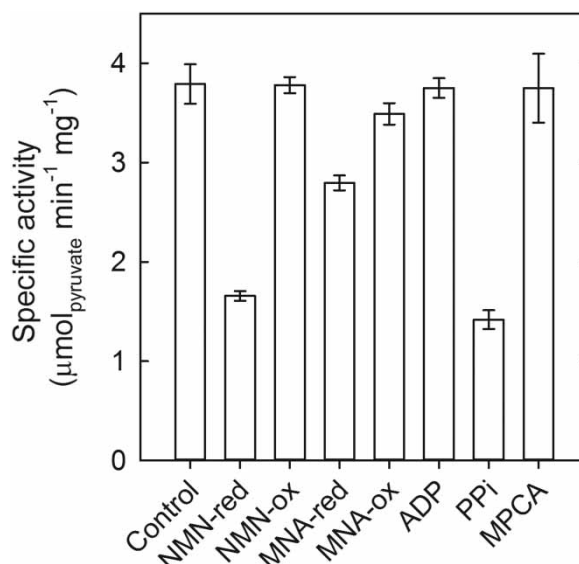


Figure 2. Effect of NADH fragments on hSR activity.

Effect of MNA-red, MNA-ox, NMN-red, NMN-ox, ADP, pyrophosphate and MPCA at a concentration of 2 mM on the β -elimination reaction of hSR in the presence of 2 mM ATP and 50 mM L-serine. Each error bar is the s.e.m. of two replicates.

KYNA, L-kynurenine, 3-HK, quinolinic acid (2,3-pyridinedicarboxylic acid, QUIN), 2-picolinic acid, XA and 3-hydroxyanthranilic acid (Supplementary Scheme S1) — were screened as potential hSR inhibitors at a concentration of 500 μ M (Supplementary Figure S3). Some of them are directly or indirectly involved in the modulation of glutamatergic transmission. KYNA acts as an orthosteric antagonist at the D-serine/glycine-binding site [29] of NMDARs, whereas QUIN acts as an agonist, causing excitotoxicity [30]. 3-HK can generate free radicals that can exacerbate QUIN-induced neuronal damage [31]. XA is an endogenous allosteric agonist of the metabotropic glutamate receptor [32] and an inhibitor of the reuptake of glutamate into the synaptic vesicles, with a K_I of 190 μ M [35]. However, no significant inhibitory activity was observed on hSR for any of the compounds tested (Supplementary Figure S4).

Determination of IC_{50} values and the inhibition mechanism

The initial rate of L-serine β -elimination by hSR was determined as a function of concentration for NADH, MNA-red and NMN-red (Figure 3) in the presence of 50 mM L-serine and 2 mM ATP. All compounds produced partial inhibition, with different residual activities at saturating concentrations. The resulting IC_{50} values were $246 \pm 63 \mu$ M for NADH, $177 \pm 63 \mu$ M for MNA-red and $51 \pm 15 \mu$ M for NMN-red. The maximum inhibition was 36% for NADH, 25% for MNA-red and 47% for NMN-red. NADH and its analogues did not produce a cumulative inhibition at saturation, suggesting a binding to the same site (Supplementary Figure S5). Preincubation with NMN-red and MNA-red with hSR did not change the level of inhibition (Supplementary Figure S6). In the absence of ATP, NADH inhibited hSR by 30%, the same extent observed in the presence of ATP (Supplementary Figure S7). This indicated that NADH acts as an inhibitor not only by competing with ATP, but also by exerting an ATP-independent allosteric modulation of hSR.

To estimate the K_I for the most active compound, NMN-red, the dependence of the initial velocity on L-serine concentration was measured in the presence of L-serine from 5 to 200 mM (Figure 4). A global fitting of the data to eqn (1) — which describes a hyperbolic mixed-type inhibition — yielded the following parameters: $K_I = 18 \pm 7 \mu$ M, $K_M = 14 \pm 3$ mM, $k_{cat} = 166 \pm 11$ min⁻¹, $\alpha = 5 \pm 2$ and $\beta = 0.8 \pm 0.1$. K_M and k_{cat} were in close agreement with those measured in a previous work [9]. The K_I calculated for NMN-red is comparable with that of 2,2-dichloromalonate, the most potent inhibitor identified so far [23]. Furthermore, an α -value higher than 1 indicated that NMN binds with higher affinity to the free enzyme in comparison with the enzyme-substrate (ES) complex. The non-zero value of the β -coefficient indicated that NMN-red behaves as a partial inhibitor. Partial inhibition takes place when the enzyme-inhibitor-substrate complex remains

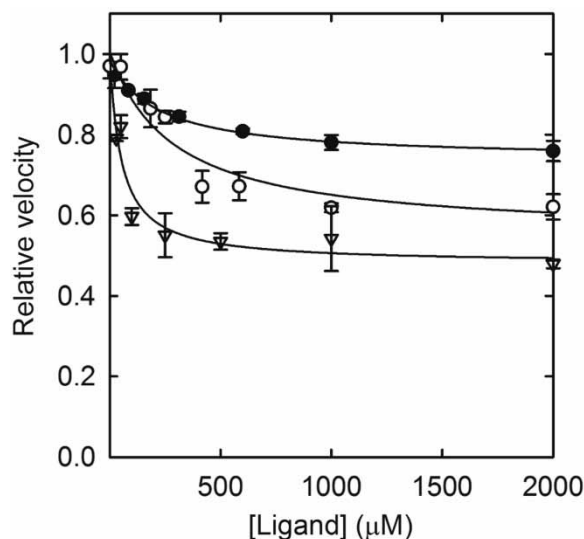


Figure 3. IC₅₀ determination.

Dependence of the β -elimination reactivity in the presence of 50 mM L-serine and 2 mM ATP-Mg²⁺ on the concentration of NADH (open circles), MNA-red (closed circles) and NMN-red (open triangles), as relative velocities in comparison with the uninhibited enzyme. The solid lines are the fitting to the equation for a binding isotherm plus an offset to account for the partial inhibition. Each error bar is the s.e.m. of two replicates. The resulting IC₅₀ values were 246 \pm 63 μ M for NADH, 177 \pm 63 μ M for MNA-red and 51 \pm 15 μ M for NMN-red.

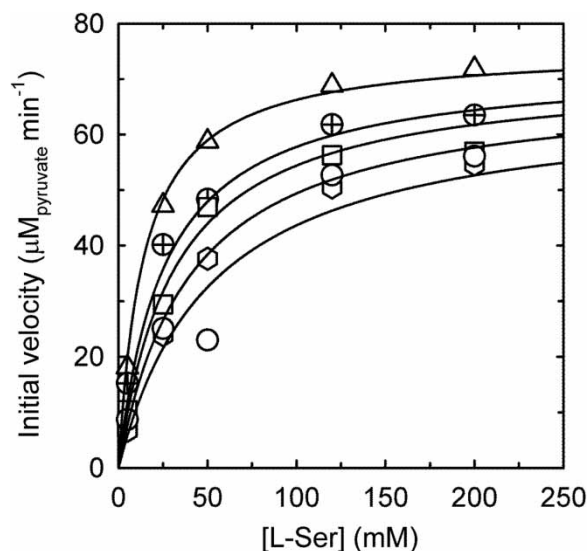


Figure 4. β -elimination activity of hSR in the presence of NMN-red at different concentrations of L-serine.

Dependence of the initial rate on L-serine concentration in the absence (triangles) and the presence of 24 (crossed circles), 40 (squares), 120 (diamonds) and 400 μ M (circles) NMN-red. The solid lines represent the global fitting to eqn (1).

catalytically active, albeit at a reduced rate relative to the ES complex [36]. Partial inhibitors are unable to completely abolish enzyme activity and, in the case of hyperbolic mixed-type inhibition, both K_M and k_{cat} are affected by the inhibitor. The nonnucleoside inhibitors of HIV reverse transcriptase are examples of clinically used partial inhibitors [37], as the fractional inhibition is enough to produce the desired therapeutic effect.

It is worth noting that the β -elimination assays reported in the literature are based on a coupled assay involving the reduction of pyruvate to lactate by LDH, in the presence of its co-substrate NADH. For a NADH concentration of 200–300 μ M, as reported in the original protocols [4], a nonnegligible inhibition of hSR could be observed, pointing to experimental biases in all reported enzyme parameters determined using this assay.

The intracellular concentration of free NAD species in the cytosol of mammalian cells is estimated to be around 300 μ M. The NAD⁺/NADH ratio heavily favours the oxidized form, which is 700-fold more concentrated than the reduced form [38]. Considering the partial inhibition and the relatively high IC₅₀, it appears unlikely that NADH could have a role in hSR modulation under physiological conditions. However, it cannot be ruled out that an altered redox state of the cell might increase the concentration of NADH to a value sufficient to exert some degree of hSR inhibition. NADPH is the prevailing form in the redox equilibrium with NADP⁺, but its cytosolic concentrations are much lower than those of NADH.

NMN is an intermediate of the salvage pathway of NADH synthesis and its concentration is also normally much lower than that of NADH [39]. However, NMN was recently shown to accumulate after nerve injury — reaching intracellular concentrations in the micromolar range — and to promote axon degeneration [33]. These findings suggested a previously unknown role of NMN and hinted at the NMN-synthesizing enzyme nicotinamide phosphoribosyltransferase as a new therapeutic target in axonopathies. Indeed, our investigation indicates that NMN binds and inhibits hSR, with a possible involvement of hSR modulation in the response to nerve injury.

Identification of the NADH-binding site

The binding site for NADH, MNA-red and NMN-red was further investigated by molecular modeling. Both the malonate-bound and -unbound dimeric structures of hSR were used for spatially unconstrained docking simulations of the identified inhibitors (NADH, NADPH, MNA-red and NMN-red). The highest docking scores for all compounds were at a pocket at the dimeric interface, where ATP binds (Supplementary Figure S8). The pocket analysis by FLAP (Fingerprint for Ligand And Protein) showed slight differences in the distribution of polar and hydrophobic environments between the pockets of the malonate-bound and -unbound structures but also between the two pseudosymmetric pockets within the same dimer [26]. Overall, the pockets appeared capable of accepting mainly H-bond donors and hydrophobic groups. The capability to receive H-bond acceptors appeared more limited.

All compounds showed a common pattern of interaction for the two conformations and between the two pseudosymmetric pockets (Figure 5). NADH and NADPH showed a comparable occupancy of the site and a good overlapping for the P-P-Ade moiety with that of ATP, the binding of which was crystallographically defined using the stable analogue 5'-adenylyl methylenediphosphonate [40] (Figure 5). The Nam moiety of all compounds positioned itself into an unoccupied hydrophobic site next to that of ATP, forming hydrogen bonds with Thr30 and Val29 (Figure 6). This secondary pocket is the binding site for MNA-red and NMN-red that thus leave most of the ATP-binding sites unoccupied (Figure 5). None of the high score poses for any of the molecules positioned the nicotinamidic ring in the adenine subsite of the ATP-binding site. For NADH, NADPH and NMN-red further bonds are formed with the ribose ring (Met278, Arg277) and the phosphate group (Ser32, Ile33) (Figure 6).

The hydrophobicity of the Nam pocket is associated with residues Phe49 and Leu29, both in close proximity to the docked ring (Figure 6). This hydrophobic environment is possibly responsible for the selectivity toward the reduced form of the Nam derivatives, as opposed to the positively charged oxidized form. Indeed, the pharmacophoric mismatch between the positively charged Nam moiety in the oxidized state and the site hydrophobicity may interfere with the protein–ligand recognition to an extent that the interaction is completely prevented.

The partial superimposition of the NADH-, NADPH- and NMN-red-binding sites with the ATP-binding site (Figure 5) might explain the observed competition (Supplementary Figure S1). However, this is not true for MNA-red, which occupies a site completely separate from that of ATP, still producing a significant, albeit reduced, inhibition. Moreover, we observed that NADH competes only partially with ATP, with a large excess of ATP incapable of restoring full activity (Supplementary Figure S1). Indeed, NADH can inhibit hSR also in the absence of ATP (Supplementary Figure S7). Therefore, a complex mechanism can be envisaged, in which NADH exerts its inhibition both by competing with the positive effector ATP and also by binding only to the Nam site, stabilizing a conformation of reduced activity even when ATP is bound. Considering that even the

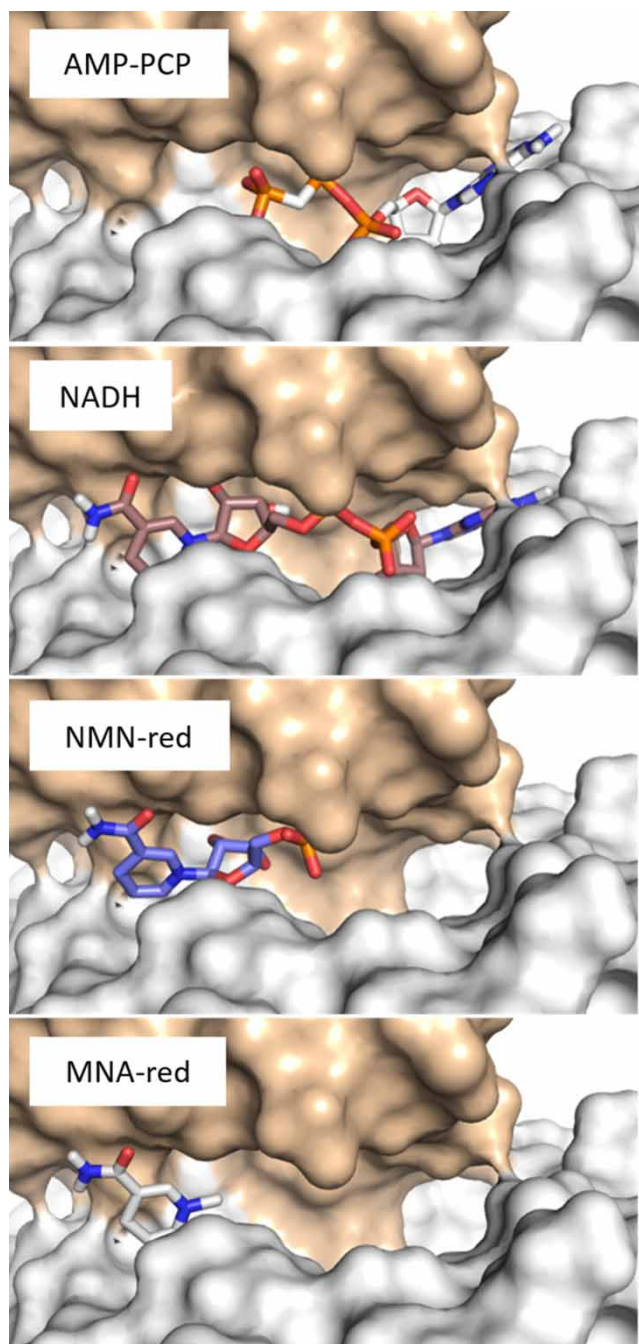


Figure 5. Binding poses of the Nam-based effectors.

Binding poses of the ATP analogue 5'-adenylyl methylenediphosphonate (AMP-PCP), NADH, MNM-red and MNA-red. Due to the global pharmacophoric analogy, only one of the two symmetry-related pockets is shown. The reported pharmacophoric profile results from the sum of the open and closed pocket pharmacophores. The pose for AMP-PCP was obtained by superimposing the structure of *Schizosaccharomyces pombe* SR-AMP-PCP complex with that of hSR. The surfaces of the two subunits are represented in a different colour.

small fragment MNA-red inhibits hSR, it can be inferred that a major contribution to the binding energy for all compounds is associated with the occupation of the Nam pocket. It can therefore be conjectured that the Nam moiety of NADH remains bound to its site when the adenine portion is displaced by ATP.

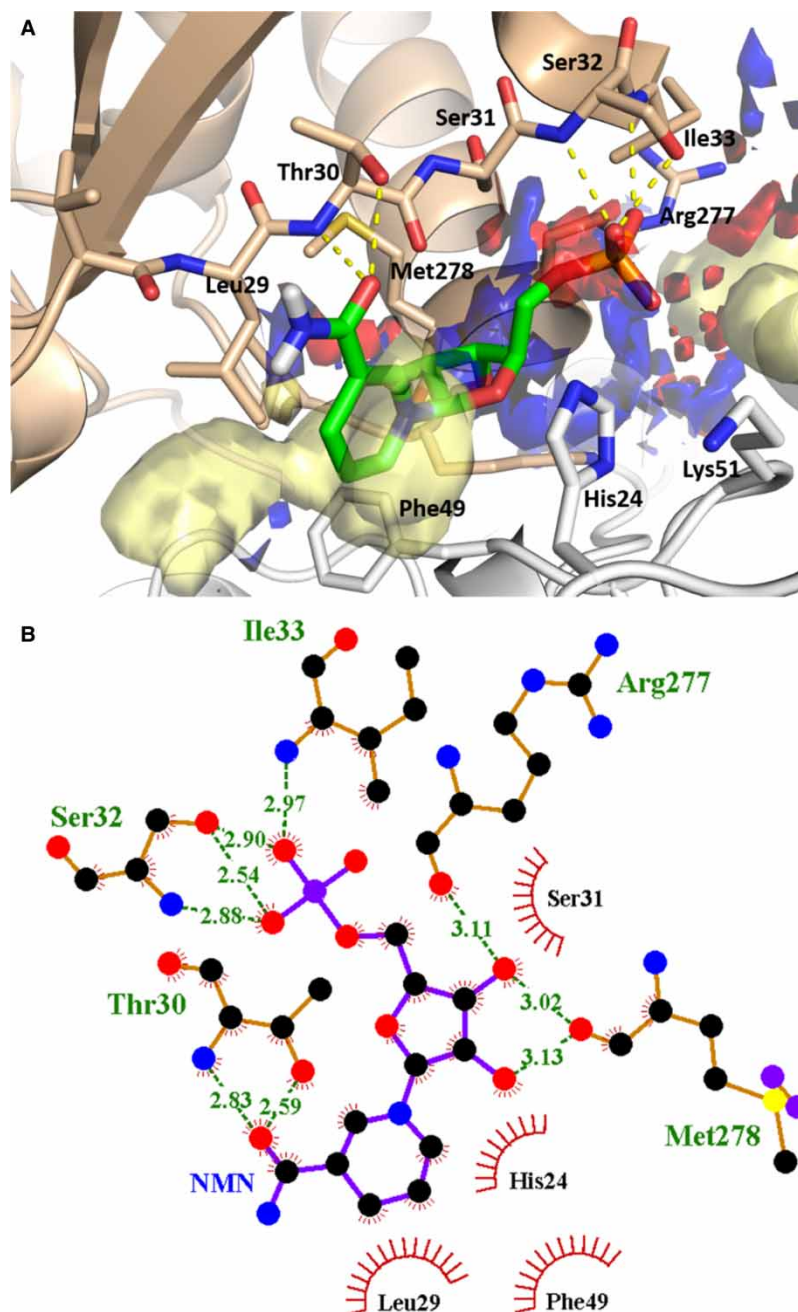


Figure 6. Close-up of NMN-red binding to hSR (A) and corresponding 2D schematic representation (B). In the 3D architecture, yellow, red and blue contours represent the favourable binding site regions for placing hydrophobic, H-bond acceptor and H-bond donor groups, respectively. The ligand and the residues in its proximity are represented by sticks. The yellow dotted lines indicate polar contacts. In the 2D representation, the dotted lines indicate polar contacts and distances are expressed in Å. The red lines represent hydrophobic contacts.

The site for the 1,4-nicotinamidic ring is a novel allosteric site that might be exploited for the fine-tuning of hSR activity. Until now, only weak inhibitors directed to the active site have been identified, particularly malonate and its derivatives. A key limitation of these inhibitors is that they are not particularly suitable for modifications, as the hSR active site is very small. The binding pocket for the 1,4-nicotinamidic ring might offer a better option for the development of more specific inhibitors endowed with higher affinity.

Materials and methods

Materials

Chemicals were of the best commercial quality available and were purchased from Sigma-Aldrich (St. Louis, MO, USA), with the exception of TCEP, from Apollo Scientific (Bredbury, UK); NADP⁺ and NADPH from Boehringer Ingelheim and 1-methyl-1,4-dihydronicotinamide (MNA-red) from Toronto Research Chemicals (Toronto, Canada). Recombinant D-amino acid oxidase (DAAO) from *Rhodotorula gracilis* was a generous gift from Professor L. Pollegioni (University of Insubria, Varese, Italy). Porcine DAAO was acquired from Sigma-Aldrich.

Enzyme preparation

Recombinant hSR was expressed as a His-tagged fusion protein encoded in a pET28a-derived plasmid [20] transformed into *Escherichia coli* BL21 CodonPlus (DE3)-RIL cells (Merck-Millipore, Darmstadt, Germany). Purification was carried out using a TALON[®] His-Tag Purification Resin (Clontech, CA, USA), as previously described [9].

Preparation of 1-methyl-1,4-dihydronicotinamide and 1,4-dihydronicotinamide mononucleotide

NMN-red was prepared from NMN-ox (Sigma-Aldrich) by stoichiometric reduction with sodium dithionite under anaerobic conditions [41], followed by desalting in an acetone:water mixture, drying in SpeedVac[™] (Thermo Scientific[™]) and resuspension in a 50% DMSO:water solution. Reduction was confirmed by ¹H NMR spectra recorded on a Bruker 400 MHz spectrometer in 20 mM Na₂HPO₄ buffer, pH 8.0 (10% D₂O), by the presence of a peak at 7.07 ppm, typical of the reduced NADH Nam ring. The concentration of the reduced species was determined spectrophotometrically based on the reported extinction coefficients [41].

hSR racemization activity assay

The initial rate of conversion of L-serine into D-serine by hSR was determined by a discontinuous assay based on the oxidation of D-serine by DAAO [9,10,42]. The assay mixture contained 50 mM TEA, 150 mM NaCl, 50 μM PLP, 50 mM L-serine and 1.5 μM hSR, unless otherwise stated. L-serine was preliminarily purified by incubation with DAAO for several hours to eliminate contaminant traces of D-serine [9]. The reaction was triggered by the addition of hSR and the mixture was periodically sampled to estimate the concentration of D-serine, as previously described [9]. Briefly, D-serine reacts with DAAO to give hydrogen peroxide, which then reacts with *o*-dianisidine in the presence of horseradish peroxidase. The absorbance of the chromophoric product was measured using a HALO LED 96 microplate reader (Dynamica) set at 550 nm.

hSR β-elimination activity assay

The initial velocity of L-serine β-elimination by hSR was monitored through a coupled assay with LDH [4,9]. The LDH-coupled assay was carried out in a solution containing 50 mM TEA, 2 mM ATP, 50 μM PLP, 5 mM DTT, 2 mM MgCl₂, 150 mM NaCl, 30 U/ml LDH and 300 μM NADH, pH 8.0, at 37°C. L-serine was added at different concentrations depending on the experiment. The reaction was triggered by the addition of 0.45 μM hSR and NADH consumption was followed at 340 nm using a Varian 4000 spectrophotometer. In some experiments, the concentrations of either NADH or ATP were modified, as specified. As NADH affects hSR activity (vide supra), its concentration was assessed spectrophotometrically at the exact time when the velocity was measured. It was therefore possible to assess reaction rates at NADH concentrations lower than those initially added for the assay.

Inhibition assays

The inhibition of either the hSR β-elimination or racemization activities by different compounds was initially evaluated at a concentration of 2 mM. For the active compounds, the IC₅₀ was determined through β-elimination assays at several inhibitor concentrations. The potential effect of each compound on the activity of the coupled enzymes LDH, DAAO and HPR was preliminarily evaluated in the presence of their substrates, that is pyruvate, D-serine and hydrogen peroxide, respectively.

The dependence of the initial rate on inhibitor concentration at different L-serine concentrations was fitted to the equation describing a hyperbolic mixed-type inhibition (eqn 1) [43]:

$$v = \frac{V_{\max}([S]/K_M) + \beta V_{\max}([S][I]/\alpha K_M K_I)}{1 + ([S]/K_M) + ([I]/K_I) + ([S][I]/\alpha K_M K_I)} \quad (1)$$

where [S] and [I] are the concentrations of L-serine and inhibitor in the assay, respectively, K_M is the Michaelis–Menten constant, α is a coefficient that indicates the difference in affinity of the inhibitor for the free enzyme and the ES complex, K_I is the inhibition constant and β is a coefficient that describes the degree of inhibition (also called efficacy). Dead-end inhibitors have $\beta = 0$.

Molecular modeling

Mammalian SRs have been crystallized in two conformations, i.e. in the presence (bound SR) and absence of the active-site ligand malonate (unbound SR), which produce the closure of the active site and a significant rotation of the small domain with respect to the large one [26]. Both conformations were used to explore putative binding sites for NADH. The model of unbound hSR was obtained by homology modeling on rat SR (PDB code 3HMK) [27], as previously reported [44]. The model of the closed structure was derived from the malonate-bound human dimer (PDB code 3L6B) [27]. The consistency of atom and bond types was checked using the software Sybyl (Tripos, version 8.1), as previously described [44]. The ligand-binding site was defined using the Flapsite tool of the FLAP software from Molecular Discovery (<http://www.moldiscovery.com>) [45], while the GRID algorithm was used to explore the pharmacophoric space. The simultaneous interaction of 1,4-dihydronicotinamide derivatives with bound and unbound hSR was investigated by docking simulations using the software GOLD [46], as previously reported [44]. No assumption about the superimposition of the adenosine moiety of NADH with the crystallographically determined pose of ATP was made in the docking simulations. No spatial constraints were used and no result improvement was obtained upon rescoring. Therefore, the native scoring function of GOLD (GOLDScore) was used. The ligand-binding poses were selected among the best scores on the basis of both the binding architecture and the match with the pharmacophore.

Abbreviations

3-HK, 3-hydroxykynurenine; ADP, adenosine diphosphate; ATP, adenosine triphosphate; DAAO, D-amino acid oxidase; KYNA, kynurenic acid; LDH, lactate dehydrogenase; MNA-ox, 1-methylnicotinamide; MNA-red, 1-methyl-1,4-dihydronicotinamide; MPCA, 1-methyl 3-piperidinecarboxamide; NAD⁺, nicotinamide adenine dinucleotide (oxidized form); NADH, nicotinamide adenine dinucleotide (reduced form); Nam, nicotinamide; NMDARs, N-methyl D-aspartate receptors; NMN-ox, β -nicotinamide mononucleotide; NMN-red, 1,4-dihydronicotinamide mononucleotide; PLP, pyridoxal 5'-phosphate; QUIN, quinolinic acid (2,3-pyridinedicarboxylic acid); SR, serine racemase; TCEP, tris(2-carboxyethyl)phosphine; TEA, triethanolamine.

Author Contribution

Stefano Bruno conceived the study and wrote the manuscript. Stefano Bruno, Andrea Mozzarelli and Barbara Campanini planned the experiments; Francesco Marchesani performed the experiments based on enzyme assays; Marilena Margiotta purified the protein; Serena Faggiano performed the NMR characterization of NADH analogues and Luca Dellafiora performed the computational analysis.

Funding

This work was partially supported by grants from the University of Parma and the Italian Ministry of University and Research (MIUR).

Competing Interests

The Authors declare that there are no competing interests associated with the manuscript.

References

- 1 Traynelis, S.F., Wollmuth, L.P., McBain, C.J., Menniti, F.S., Vance, K.M., Ogden, K.K. et al. (2010) Glutamate receptor ion channels: structure, regulation, and function. *Pharmacol. Rev.* **62**, 405–496 doi:10.1124/pr.109.002451

- 2 Wolosker, H., Blackshaw, S. and Snyder, S.H. (1999) Serine racemase: a glial enzyme synthesizing D-serine to regulate glutamate-N-methyl-D-aspartate neurotransmission. *Proc. Natl Acad. Sci. USA* **96**, 13409–13414 doi:10.1073/pnas.96.23.13409
- 3 de Miranda, J., Panizzutti, R., Foltyn, V.N. and Wolosker, H. (2002) Cofactors of serine racemase that physiologically stimulate the synthesis of the N-methyl-D-aspartate (NMDA) receptor coagonist D-serine. *Proc. Natl Acad. Sci. USA* **99**, 14542–14547 doi:10.1073/pnas.222421299
- 4 Foltyn, V.N., Bendikov, I., De Miranda, J., Panizzutti, R., Dumin, E., Shleper, M. et al. (2005) Serine racemase modulates intracellular D-serine levels through an alpha,beta-elimination activity. *J. Biol. Chem.* **280**, 1754–1763 doi:10.1074/jbc.M405726200
- 5 Foltyn, V.N., Zehl, M., Dikopoltsev, E., Jensen, O.N. and Wolosker, H. (2010) Phosphorylation of mouse serine racemase regulates D-serine synthesis. *FEBS Lett.* **584**, 2937–2941 doi:10.1016/j.febslet.2010.05.022
- 6 Hoffman, H.E., Jiraskova, J., Ingr, M., Zvelebil, M. and Konvalinka, J. (2009) Recombinant human serine racemase: enzymologic characterization and comparison with its mouse ortholog. *Protein Expr. Purif.* **63**, 62–67 doi:10.1016/j.pep.2008.09.003
- 7 Campanini, B., Spyrikis, F., Peracchi, A. and Mozzarelli, A. (2013) Serine racemase: a key player in neuron activity and in neuropathologies. *Front. Biosci. (Landmark Ed.)* **18**, 1112–1128 doi:10.2741/4167
- 8 Canu, N., Ciotti, M.T. and Pollegioni, L. (2014) Serine racemase: a key player in apoptosis and necrosis. *Front. Synaptic Neurosci.* **6**, 9 doi:10.3389/fnsyn.2014.00009
- 9 Marchetti, M., Bruno, S., Campanini, B., Peracchi, A., Mai, N. and Mozzarelli, A. (2013) ATP binding to human serine racemase is cooperative and modulated by glycine. *FEBS J.* **280**, 5853–5863 doi:10.1111/febs.12510
- 10 Sacchi, S., Caldinelli, L., Cappelletti, P., Pollegioni, L. and Molla, G. (2012) Structure-function relationships in human D-amino acid oxidase. *Amino Acids* **43**, 1833–1850 doi:10.1007/s00726-012-1345-4
- 11 Ding, X., Ma, N., Nagahama, M., Yamada, K. and Semba, R. (2011) Localization of D-serine and serine racemase in neurons and neuroglia in mouse brain. *Neurosci. Sci.* **32**, 263–267 doi:10.1007/s10072-010-0422-2
- 12 Benneyworth, M.A., Li, Y., Basu, A.C., Bolshakov, V.Y. and Coyle, J.T. (2012) Cell selective conditional null mutations of serine racemase demonstrate a predominate localization in cortical glutamatergic neurons. *Cell Mol. Neurobiol.* **32**, 613–624 doi:10.1007/s10571-012-9808-4
- 13 Montesinos Guevara, C. and AR, M. (2016) The role of D-serine in peripheral tissues. *Eur. J. Pharmacol.* doi:10.1016/j.ejphar.2016.03.054
- 14 Paoletti, P. and Neyton, J. (2007) NMDA receptor subunits: function and pharmacology. *Curr. Opin. Pharmacol.* **7**, 39–47 doi:10.1016/j.coph.2006.08.011
- 15 Molla, G., Sacchi, S., Bernasconi, M., Pilone, M.S., Fukui, K. and Pollegioni, L. (2006) Characterization of human D-amino acid oxidase. *FEBS Lett.* **580**, 2358–2364 doi:10.1016/j.febslet.2006.03.045
- 16 Lipton, S.A. (2006) Paradigm shift in neuroprotection by NMDA receptor blockade: memantine and beyond. *Nat. Rev. Drug Discov.* **5**, 160–170 doi:10.1038/nrd1958
- 17 Conti, P., Tamborini, L., Pinto, A., Blondel, A., Minoprio, P., Mozzarelli, A. et al. (2011) Drug discovery targeting amino acid racemases. *Chem. Rev.* **111**, 6919–6946 doi:10.1021/cr2000702
- 18 Amadasi, A., Bertoldi, M., Contestabile, R., Bettati, S., Cellini, B., di Salvo, M.L. et al. (2007) Pyridoxal 5'-phosphate enzymes as targets for therapeutic agents. *Curr. Med. Chem.* **14**, 1291–1324 doi:10.2174/092986707780597899
- 19 Hoffman, H.E., Jirásková, J., Cigler, P., Šanda, M., Schraml, J. and Konvalinka, J. (2009) Hydroxamic acids as a novel family of serine racemase inhibitors: mechanistic analysis reveals different modes of interaction with the pyridoxal-5'-phosphate cofactor. *J. Med. Chem.* **52**, 6032–6041 doi:10.1021/jm900775q
- 20 Dixon, S.M., Li, P., Liu, R., Wolosker, H., Lam, K.S., Kurth, M.J. et al. (2006) Slow-binding human serine racemase inhibitors from high-throughput screening of combinatorial libraries. *J. Med. Chem.* **49**, 2388–2397 doi:10.1021/jm050701c
- 21 Jiraskova-Vanickova, J., Ettrich, R., Vorlova, B., Hoffman, H.E., Lepsik, M., Jansa, P. et al. (2011) Inhibition of human serine racemase, an emerging target for medicinal chemistry. *Curr. Drug Targets* **12**, 1037–1055 doi:10.2174/138945011795677755
- 22 Strišovský, K., Jirásková, J., Mikulová, A., Rulišek, L. and Konvalinka, J. (2005) Dual substrate and reaction specificity in mouse serine racemase: identification of high-affinity dicarboxylate substrate and inhibitors and analysis of the β -eliminase activity. *Biochemistry* **44**, 13091–13100 doi:10.1021/bi051201o
- 23 Vorlová, B., Nachtigallová, D., Jirásková-Vaničková, J., Ajani, H., Jansa, P., Řezáč, J. et al. (2015) Malonate-based inhibitors of mammalian serine racemase: kinetic characterization and structure-based computational study. *Eur. J. Med. Chem.* **89**, 189–197 doi:10.1016/j.ejmech.2014.10.043
- 24 Mori, H., Wada, R., Li, J., Ishimoto, T., Mizuguchi, M., Obita, T. et al. (2014) In silico and pharmacological screenings identify novel serine racemase inhibitors. *Bioorg. Med. Chem. Lett.* **24**, 3732–3735 doi:10.1016/j.bmcl.2014.07.003
- 25 Beato, C., Pecchini, C., Cocconcelli, C., Campanini, B., Marchetti, M., Pieroni, M. et al. (2016) Cyclopropane derivatives as potential human serine racemase inhibitors: unveiling novel insights into a difficult target. *J. Enzyme Inhib. Med. Chem.* **31**:645–652 doi:10.3109/14756366.2015.1057720
- 26 Dellafiora, L., Marchetti, M., Spyrikis, F., Orlandi, V., Campanini, B., Cruciani, G. et al. (2015) Expanding the chemical space of human serine racemase inhibitors. *Bioorg. Med. Chem. Lett.* **25**:4297–4303 doi:10.1016/j.bmcl.2015.07.081
- 27 Smith, M.A., Mack, V., Ebnet, A., Moraes, I., Felicetti, B., Wood, M. et al. (2010) The structure of mammalian serine racemase: evidence for conformational changes upon inhibitor binding. *J. Biol. Chem.* **285**, 12873–12881 doi:10.1074/jbc.M109.050062
- 28 Suzuki, M., Sasabe, J., Miyoshi, Y., Kuwasako, K., Muto, Y., Hamase, K. et al. (2015) Glycolytic flux controls D-serine synthesis through glyceraldehyde-3-phosphate dehydrogenase in astrocytes. *Proc. Natl Acad. Sci. USA* **112**, E2217–E2224 doi:10.1073/pnas.1416117112
- 29 Schwarcz, R., Bruno, J.P., Muchowski, P.J. and Wu, H.-Q. (2012) Kynurenes in the mammalian brain: when physiology meets pathology. *Nat. Rev. Neurosci.* **13**, 465–477 doi:10.1038/nrn3257
- 30 Lugo-Huitron, R., Ugalde Muniz, P., Pineda, B., Pedraza-Chaverri, J., Rios, C. and Perez-de la Cruz, V. (2013) Quinolinic acid: an endogenous neurotoxin with multiple targets. *Oxid. Med. Cell Longev.* **2013**, 104024 doi:10.1155/2013/104024
- 31 Stone, T.W. and Darlington, L.G. (2002) Endogenous kynurenes as targets for drug discovery and development. *Nat. Rev. Drug Discov.* **1**, 609–620 doi:10.1038/nrd870
- 32 Copeland, C.S., Neale, S.A. and Salt, T.E. (2013) Actions of xanthurenic acid, a putative endogenous group II metabotropic glutamate receptor agonist, on sensory transmission in the thalamus. *Neuropharmacology* **66**, 133–142 doi:10.1016/j.neuropharm.2012.03.009

- 33 Di Stefano, M., Nascimento-Ferreira, I., Orsomando, G., Mori, V., Gilley, J., Brown, R. et al. (2015) A rise in NAD precursor nicotinamide mononucleotide (NMN) after injury promotes axon degeneration. *Cell Death Differ.* **22**, 731–742 doi:10.1038/cdd.2014.164
- 34 Marchetti, M., Bruno, S., Campanini, B., Bettati, S., Peracchi, A. and Mozzarelli, A. (2015) Regulation of human serine racemase activity and dynamics by halides, ATP and malonate. *Amino Acids* **47**, 163–173 doi:10.1007/s00726-014-1856-2
- 35 Bartlett, R.D., Esslinger, C.S., Thompson, C.M. and Bridges, R.J. (1998) Substituted quinolines as inhibitors of L-glutamate transport into synaptic vesicles. *Neuropharmacology* **37**, 839–846 doi:10.1016/S0028-3908(98)00080-X
- 36 Copeland, R.A. (2000) *Enzymes: A Practical Introduction to Structure, Mechanism, and Data Analysis*, Wiley-VCH, Inc
- 37 Spence, R.A., Kati, W.M., Anderson, K.S. and Johnson, K.A. (1995) Mechanism of inhibition of HIV-1 reverse transcriptase by nonnucleoside inhibitors. *Science* **267**, 988–993 doi:10.1126/science.7532321
- 38 Ying, W. (2008) NAD⁺/NADH and NADP⁺/NADPH in cellular functions and cell death: regulation and biological consequences. *Antioxid. Redox Signal.* **10**, 179–206 doi:10.1089/ars.2007.1672
- 39 Magni, G., Amici, A., Emanuelli, M., Orsomando, G., Raffaelli, N. and Ruggieri, S. (2004) Enzymology of NAD⁺ homeostasis in man. *Cell Mol. Life Sci.* **61**, 19–34 doi:10.1007/s00018-003-3161-1
- 40 Goto, M., Yamauchi, T., Kamiya, N., Miyahara, I., Yoshimura, T., Mihara, H. et al. (2009) Crystal structure of a homolog of mammalian serine racemase from *Schizosaccharomyces pombe*. *J. Biol. Chem.* **284**, 25944–25952 doi:10.1074/jbc.M109.010470
- 41 Blankenhorn, G. and Moore, E.G. (1980) Sulfoxylate ion (HSO₂⁻), the hydride donor in dithionite-dependent reduction of NAD⁺ analogs. *J. Am. Chem. Soc.* **102**, 1092–1098 doi:10.1021/ja00523a028
- 42 Molla, G., Piubelli, L., Volonte, F. and Pilone, M.S. (2012) Enzymatic detection of D-amino acids. *Methods Mol. Biol.* **794**, 273–289 doi:10.1007/978-1-61779-331-8_18
- 43 Segel, H.I. (1993) *Enzyme Kinetics: Behavior and Analysis of Rapid Equilibrium and Steady-State Enzyme Systems*, Wiley
- 44 Dellafiora, L., Dall'Asta, C. and Cozzini, P. (2015) Ergot alkaloids: from witchcraft till in silico analysis. Multi-receptor analysis of ergotamine metabolites. *Toxicol. Rep.* **2**, 535–545 doi:10.1016/j.toxrep.2015.03.005
- 45 Baroni, M., Cruciani, G., Sciabola, S., Perruccio, F. and Mason, J.S. (2007) A common reference framework for analyzing/comparing proteins and ligands. Fingerprints for ligands and proteins (FLAP): theory and application. *J. Chem. Inf. Model* **47**, 279–294 doi:10.1021/ci600253e
- 46 Verdonk, M.L., Cole, J.C., Hartshorn, M.J., Murray, C.W. and Taylor, R.D. (2003) Improved protein-ligand docking using GOLD. *Proteins* **52**, 609–623 doi:10.1002/prot.10465